

Amableite-(Ce), $\text{Na}_{15}[(\text{Ce}_{1.5}\text{Na}_{1.5})\text{Mn}_3]\text{Mn}_2\text{Zr}_3\text{Si}[\text{Si}_{24}\text{O}_{69}(\text{OH})_3](\text{OH})_2\cdot\text{H}_2\text{O}$, a new eudialyte-group mineral from Saint-Amable Sill, Québec, Canada

NIKITA V. CHUKANOV^{1,2*}, ANDREY A. ZOLOTAREV³, CHRISTOF SCHÄFER⁴, DMITRY A. VARLAMOV⁵, IGOR V. PEKOV², MARINA F. VIGASINA², DMITRY I. BELAKOVSKIY⁸, SERGEY M. AKSENOV^{6,7}, SVETLANA A. VOZCHIKOVA¹, SERGEY N. BRITVIN³

¹ Federal Research Center of Problems of Chemical Physics and Medicinal Chemistry, Russian Academy of Sciences, Chernogolovka, Moscow region, 142432 Russia

² Faculty of Geology, Moscow State University, Vorobievsky Gory, 119991 Moscow, Russia

³ Department of Crystallography, St. Petersburg State University, University Emb. 7/9, Saint-Petersburg 199034, Russia

⁴ Gustav Stresemann-Strasse 34, 74257 Untereisesheim, Germany

⁵ Institute of Experimental Mineralogy RAS, Chernogolovka, 142432 Russia

⁶ Laboratory of Arctic Mineralogy and Material Sciences, Kola Science Centre, Russian Academy of Sciences, 14 Fersman str., Apatity 184209 Russia

⁷ Geological Institute, Kola Science Centre, Russian Academy of Sciences, 14 Fersman str., Apatity 184209 Russia

⁸ Fersman Mineralogical Museum of the Russian Academy of Sciences, Leninsky Prospekt 18-2, 119071 Moscow, Russia

*E-mail: chukanov@icp.ac.ru

Running title: Amableite-(Ce), a new mineral



This is a 'preproof' accepted article for Mineralogical Magazine. This version may be subject to change during the production process.
DOI: 10.1180/mgm.2024.26

Abstract

The new eudialyte-group mineral amableite-(Ce), ideally $\text{Na}_{15}[(\text{Ce}_{1.5}\text{Na}_{1.5})\text{Mn}_3]\text{Mn}_2\text{Zr}_3\text{Si}[\text{Si}_{24}\text{O}_{69}(\text{OH})_3](\text{OH})_2\cdot\text{H}_2\text{O}$, was discovered in a peralkaline pegmatite at Saint-Amable Sill, Montérégie, Québec, Canada. The associated minerals are albite, microcline, aegirine, sérandite, an natrolite, yofortierite, and an unidentified titanosilicate forming minute grains. Amableite-(Ce) occurs as yellow equant or thick tabular crystals up to 2 mm across. The observed crystal forms are $\{0001\}$; the subordinate forms are $\{11\text{-}20\}$, $\{10\text{-}11\}$, and $\{10\text{-}10\}$. Amableite-(Ce) is brittle, with the Mohs' hardness of 5. $D(\text{meas}) = 2.89(1)$, $D(\text{calc}) = 2.899 \text{ g}\cdot\text{cm}^{-3}$. Amableite-(Ce) is optically anomalously biaxial, positive with $\alpha \approx \beta = 1.603(2)$ and $\gamma = 1.608(2)$. The chemical composition is (wt.%, electron microprobe, H_2O measured by means of a modified Penfield method): Na_2O 14.20, K_2O 0.41, CaO 1.89, MnO 8.25, Fe_2O_3 2.40, La_2O_3 3.10, Ce_2O_3 4.19, Pr_2O_3 0.16, Nd_2O_3 0.59, SiO_2 49.41, ZrO_2 11.17, HfO_2 0.24, TiO_2 0.68, Nb_2O_5 1.54, Cl 0.26, H_2O 1.70, $-\text{O}\equiv\text{Cl}$ -0.06 , total 100.13. The crystal structure was determined using single-crystal X-ray diffraction data and refined to $R1 = 0.0423$. Amableite-(Ce) is trigonal, space group $R\bar{3}$, with $a = 14.1340(3) \text{ \AA}$, $c = 30.3780(11) \text{ \AA}$ and $V = 5255.6(3) \text{ \AA}^3$. The crystal-chemical formula is $(\text{Na}_{12.93}\text{K}_{0.27}\text{Ce}_{0.06})[(\text{Mn}_{2.49}\text{Ce}_{0.30}\text{Ca}_{0.21})(\text{Ce}_{1.14}\text{Na}_{1.04}\text{Ca}_{0.82})](\text{Mn}_{1.05}\text{Fe}_{0.90}\square_{1.05})(\text{Zr}_{2.85}\text{Ti}_{0.12}\text{Hf}_{0.03})(\square_{0.40}\text{Nb}_{0.36}\text{Si}_{0.24})(\text{Si}_{0.88}\square_{0.12})[\text{Si}_{24}(\text{O}_{70.44}(\text{OH})_{1.56})][(\text{OH})_{2.20}(\text{H}_2\text{O})_{1.27}]\text{Cl}_{0.22}$ ($Z = 3$). Infrared and Raman spectra are given. The strongest lines of the powder X-ray diffraction pattern [d , Å (I , %)] (hkl) are: 11.34 (51) (101), 7.06 (76) (110), 4.312 (63) (205), 3.783 (38) (033), 3.538 (43) (027, 220), 2.963 (84) (-345), 2.837 (100) (404). The mineral is named after the discovery locality.

Keywords: amableite-(Ce); new mineral; eudialyte group; crystal structure; IR spectroscopy; Raman spectroscopy; X-ray diffraction; Saint-Amable Sill; Canada.

Introduction

Eudialyte-group minerals (EGMs) are important components of some kinds of peralkaline rocks in which they are the main concentrators of zirconium. Currently, 32 mineral species belonging to the eudialyte group are known. Their crystal structures are based on heteropolyhedral frameworks composed of nine- and three-membered rings of SiO_4 tetrahedra, six-membered rings of edge-sharing $M1\text{O}_6$ octahedra and isolated $Z\text{O}_6$ octahedra. The simplified general formula of EGMs is $[N1N2N3N4N5]_3M1_6M2_3M3M4Z_3(\text{Si}_9\text{O}_{27})_2(\text{Si}_3\text{O}_9)_2\text{O}_{4-6}X1X2$ where $N1-5$ are extra-framework cations (mainly, Na^+ or H_3O^+ , sometimes with species-defining H_2O , K^+ , Ca^{2+} , Sr^{2+} , Mn^{2+} or REE^{3+} as well as minor H^+ and/or Ba^{2+}); $M1 = \text{Ca}^{2+}$, Na^+ , Fe^{2+} , Mn^{2+} , REE^{3+} ; $M2 = \text{Na}^+$, Fe^{2+} , Mn^{2+} , Fe^{3+} or Zr occurring between rings of $M1\text{O}_6$ octahedra; $M3$ and $M4$ are $^{[4]}\text{Si}$, $^{[4]}\text{Nb}$, $^{[4]}\text{W}$ or $^{[4]}\text{Ti}$ atoms occurring at the centers of the Si_9O_{27} rings; $Z = \text{Zr}$ or Ti ; O , $X1$ and $X2$ are additional extra-framework anions (OH^- , Cl^- , F^- , O^{2-} , CO_3^{2-} , SO_4^{2-} , S^{2-}) and water molecules (Johnsen *et al.*, 2003; Rastsvetaeva *et al.* 2012). All sites except those belonging to the rings of tetrahedral and octahedra can be partly vacant. Most EGMs are characterized by the space groups $R\bar{3}m$ or $R3m$, but in some species (members of the oneillite subgroup) different $M1$ -cations are ordered in the $M1(1)$ and $M1(2)$ sites alternating in the six-membered rings of octahedra which results in lowering of symmetry from $R\bar{3}m$ or $R3m$ to $R3$ Johnsen *et al.*, 1999; Chukanov *et al.*, 2003, 2020, 2022, 2023; Khomyakov *et al.*, 2007, 2009).

This paper describes a new oneillite-subgroup member amableite-(Ce), with $\text{Na}^+ + \text{REE}^{3+}$ and Mn^{2+} ordered in the in the $M1(1)$ and $M1(2)$ sites and Mn^{2+} -dominant $M2$ site. Amableite-(Ce) is named after its discovery locality, Saint-Amable Sill. The mineral and its name have been approved by the IMA Commission on New Minerals, Nomenclature and Classification (IMA No. 2023-075). The holotype specimen is deposited in the Fersman Mineralogical Museum of the Russian Academy of Sciences, Moscow, Russia with the registration number 6921/1.

Experimental methods and data processing

In order to obtain IR absorption spectra of amableite-(Ce) and related eudialyte-group mineral voronkovite (Khomyakov *et al.*, 2009), powdered samples were mixed with anhydrous KBr, pelletized, and analyzed using an ALPHA FTIR spectrometer (Bruker Optics) at a resolution of 4 cm^{-1} . A total of 16 scans were collected. The IR spectrum of an analogous pellet of pure KBr was used as a reference. The assignment of IR bands was made based on the analysis of IR spectra of several tens structurally investigated eudialyte-group minerals, in accordance with Rastsvetaeva *et al.* (2012).

Raman spectra of a randomly oriented grains of amabelite-(Ce) and other eudialyte-group minerals used for comparison were obtained using an EnSpectr R532 spectrometer based on an OLYMPUS CX 41 microscope coupled with a diode laser ($\lambda = 532\text{ nm}$) at room temperature (Moscow State University, Faculty of Geology). The spectra were recorded in the range from 100 to 4000 cm^{-1} with a diffraction grating (1800 gr mm^{-1}) and spectral resolution about 6 cm^{-1} . The output power of the laser beam was in the range from 5 to 13 mW. The diameter of the focal spot on the sample was 5 – 10 μm . The backscattered Raman signal was collected with a $40\times$ objective; signal acquisition time for a single scan of the spectral range was 1 s, and the signal was averaged over 50 scans. Crystalline silicon was used as a standard.

Chemical data (5 spot analyses) were carried out using a digital scanning electron microscope Tescan VEGA-II XMU equipped by energy-dispersive spectrometer (EDS) INCA Energy 450 with semiconducting Si (Li) detector Link INCA Energy at an accelerating voltage of 20 kV, electron current of 190 pA and electron beam diameter of 160–180 nm. Attempts to use WDS mode, with a higher beam current, were unsuccessful because of instability of the mineral under electron beam due to partial dehydration and migration of Na. This phenomenon is typical for high-hydrated sodium minerals with microporous structures. A good agreement was observed between compositional data obtained under these standard conditions and those obtained under more “mild” conditions (with a current lowered to 90 – 100 pA and electron beam defocused to an

area of 30×30 μm). The *L*-lines of Ta are not observed in the spectrum, which indicates the absence of detectable amounts of tantalum in amableite-(Ce).

The H₂O content was determined by means of a modified Penfield method. The CO₂ content was not determined because characteristic bands of carbonate groups (in the range of 1350 – 1550 cm⁻¹) are not observed in the IR spectrum of amableite-(Ce).

Powder X-ray diffraction data were collected using a Rigaku R-Axis Rapid II diffractometer (image plate), CoKα, 40 kV, 15 mA, rotating anode with the microfocus optics, Debye-Scherrer geometry, *d* = 127.4 mm, exposure 15 min. The raw powder XRD data were collected using program suite designed by Britvin *et al.* (2017). Calculated intensities were obtained by means of STOE WinXPOW v. 2.08 program suite based on the atomic coordinates and unit-cell parameters (Stoe, 2003).

Single-crystal X-ray diffraction studies were carried out using a Rigaku XtaLAB Synergy-S diffractometer (MoKα radiation) with high-stability sharp-focus X-ray source PhotonJet-S and a high-speed direct-action detector HyPix-6000HE. The CrysAlisPro software was used for further processing (CrysAlisPro, 2015). An absorption correction was introduced using the SCALE3 ABSPACK algorithm. The obtained data were loaded into the Olex2 program software (Dolmatov *et al.*, 2009) and the crystal structure was solved and refined by the ShelX program package (Sheldrick, 2015). The crystal data, experimental details of the data collection and refinement results are shown in Table 1.

Results

Occurrence, General Appearance and Physical Properties

The material with amableite-(Ce) was collected in the Demix-Varenes quarry, Saint-Amable Sill (45° 40' 1" N, 73° 20' 35" W), Lajemmerais RCM, Montérégie, Québec, Canada (see: Horváth *et*

al., 1998). Amabelite-(Ce) crystallized from a peralkaline post-magmatic fluid. It forms yellow thick-tabular, slightly flattened on (0001) crystals up to 2 mm across in cavities of peralkaline pegmatite (Fig. 1). The dominant crystal form is {0001}; the subordinate forms are {11-20}, {10-11}, and {10-10}. The associated minerals are albite, microcline, aegirine, sérandite, an natrolite, yofortierite, and an unidentified titanosilicate forming minute grains.



Fig. 1. Amableite-(Ce) crystals (yellow) in association with albite, aegirine and natrolite. FOV width is 3.5 mm. Photographer: V. Heck.

Amableite-(Ce) is brittle, with the Mohs' hardness of 5. No cleavage is observed. The fracture is uneven. Density measured by flotation in heavy liquids (mixtures of methylene iodide and heptane) is equal to $2.89(1) \text{ g}\cdot\text{cm}^{-3}$. Density calculated using the empirical formula and unit-cell volume refined from single-crystal XRD data is $2.90 \text{ g}\cdot\text{cm}^{-3}$.

The new mineral is optically anomalously biaxial, positive with $\alpha \approx \beta = 1.603(2)$ and $\gamma = 1.608(2)$ ($\lambda = 589 \text{ nm}$). Different causes of optical anomalies (microstrains, compositional inhomogeneity, including different degree of dehydration in different zones or sectors *etc.*) are discussed in detail by Shtukenberg and Punin (2007). A possible cause of optical anomalies may be deformation of the crystals during their growth or when they were crushing. In particular,

anomalous biaxiality is very typical for eudialyte-group minerals despite all studied members of this group are trigonal (Rastsvetaeva *et al.*, 2012). Under the microscope, amableite-(Ce) is colourless, nonpleochroic. Dispersion is distinct, $r > v$.

Infrared spectroscopy

Absorption bands in the IR spectrum of amableite-(Ce) (curve *a* in Fig. 2) and their assignments are (cm^{-1} ; s – strong band, w – weak band, sh – shoulder): 3520, 3335, 2880w (O–H stretching vibrations), 1635w (H–O–H bending vibrations), 1170sh 1010s, 991s (Si–O stretching vibrations of silicate rings), 935s (Si–O stretching vibrations of SiO_4 tetrahedra at the *M3* and *M4* sites), 739 (mixed vibrations of rings of SiO_4 tetrahedra – “ring band”), 700sh, 657 (mixed vibrations of rings of SiO_4 tetrahedra combined with Nb–O stretching vibrations), 519sh ($^{\text{IV}}\text{Mn}^{2+}$ –O and/or $^{\text{V}}\text{Fe}^{3+}$ –O stretching vibrations), 481s, 446s (lattice mode involving predominantly bending vibrations of rings of SiO_4 tetrahedra), 390sh, 373 (lattice modes involving $^{\text{VI}}(\text{Ca}, \text{Mn}^{2+})$ –O stretching vibrations).

The band of $^{\text{IV}}\text{Fe}^{2+}$ –O stretching vibrations (in the range 539 – 545 cm^{-1}) is not observed. The IR spectrum of amableite-(Ce) differs from that of the related eudialyte-group mineral voronkovite, ideally $\text{Na}_{15}[(\text{Na}, \text{Ca})_3\text{Mn}_3]\text{Fe}^{2+}_3\text{Zr}_3\text{Si}_2(\text{Si}_{24}\text{O}_{72})(\text{OH}, \text{O})_4\text{Cl}\cdot\text{H}_2\text{O}$ (curve *b* in Figure 2), in a lower intensity of the band at 933 – 935 cm^{-1} which reflects significant amounts of vacancies and Nb at the *M3* and *M4* sites, in accordance with the structural data (see below).

According to the correlation by Libowitzky (1999), the band of O–H stretching vibrations with the maximum at 3335 cm^{-1} corresponds to a hydrogen bond with the $\text{O}\cdots\text{O}$ distance of 2.72 Å. Thus, this band should be assigned to the hydrogen bond $\text{O}_{24}\cdots\text{H}-\text{O}_{26}$ with the $\text{O}\cdots\text{O}$ distance of 2.72(3) Å. The band at 3520 cm^{-1} may correspond to silanol groups formed as a result of protonation of pending vertices of the SiO_4 tetrahedra, but this assignment is ambiguous because H atoms were not localized.

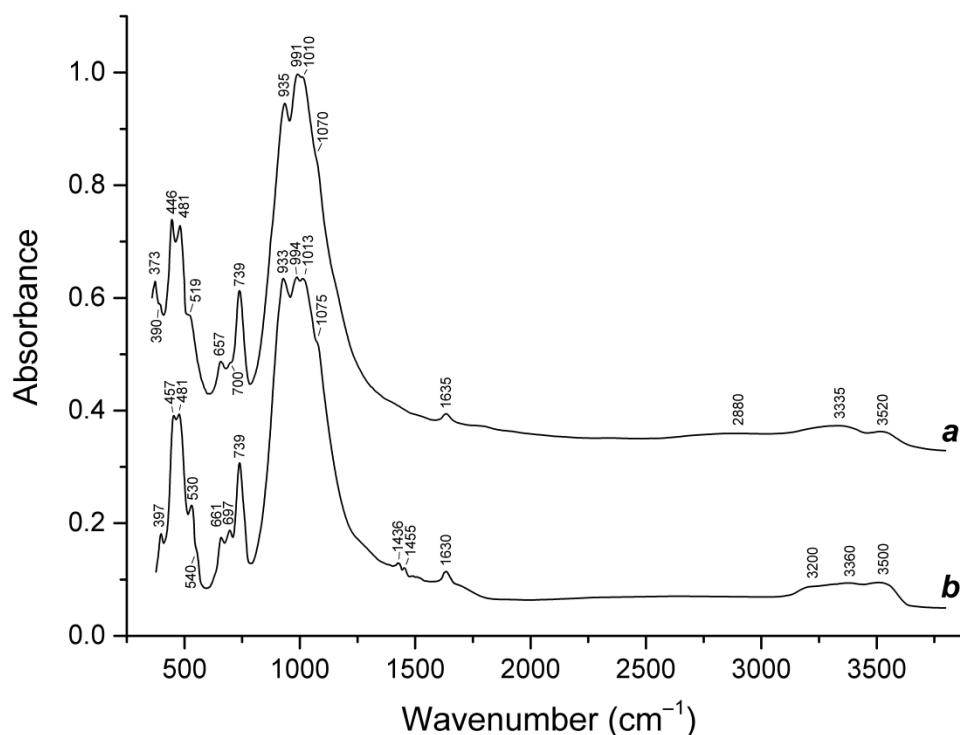


Fig. 2. Powder infrared absorption spectra of (a) amableite-(Ce) and (b) holotype sample of voronkovite (Khomyakov *et al.*, 2009), an oneillite-type EGM related to amableite-(Ce). The spectra are offset for comparison.

Raman spectroscopy

A specific feature of Raman spectra of the EGMs selsurtite, ideally $(\text{H}_3\text{O})_{12}\text{Na}_3(\text{Ca}_3\text{Mn}_3)(\text{Na}_2\text{Fe})\text{Zr}_3\text{Si}[\text{Si}_{24}\text{O}_{69}(\text{OH})_3](\text{OH})\text{Cl}\cdot\text{H}_2\text{O}$ (Chukanov *et al.*, 2023), aqualite, ideally $(\text{H}_3\text{O})_9(\text{K},\text{Ba},\text{Sr})_2\text{Ca}_6\text{Zr}_3\text{Na}_2\text{Si}_2[\text{Si}_{24}\text{O}_{66}(\text{OH})_6](\text{OH})_3\text{Cl}\cdot\text{H}_2\text{O}$ (Khomyakov *et al.*, 2007) and other hydronium-bearing EGMs is a series of bands in the range of $1200 - 2900 \text{ cm}^{-1}$ corresponding to strong hydrogen bonds formed by hydronium cations in different local situations including Zundel- and Eigen-like ones with short $\text{O}\cdots\text{O}$ distances of ~ 2.4 and $\sim 2.6 \text{ \AA}$ (Chukanov *et al.*, 2022, 2023; see Discussion section for details). Similar but much weaker bands are observed in the Raman spectrum of amableite-(Ce), but such bands are absent in the Raman spectrum of eudialyte which does not contain hydrated proton complexes including $(\text{H}_3\text{O})^+$ cation groups (Fig. 3). Most probably, hydrated protons could form as a result of partial dissociation of silanol (SiOH) groups.

The assignment of other bands in the Raman spectrum of amableite-(Ce) is as follows.

3430 cm^{-1} – O–H stretching vibrations of H_2O molecules and/or OH groups.

The range 900 – 1300 cm^{-1} – Si–O stretching modes.

780 cm^{-1} – mixed vibrations of rings of SiO_4 tetrahedra.

653 and 689 cm^{-1} – mixed vibrations of rings of SiO_4 tetrahedra combined with Nb–O stretching vibrations.

573 cm^{-1} – Zr–O stretching vibrations.

$\leq 400 \text{ cm}^{-1}$ – lattice modes.

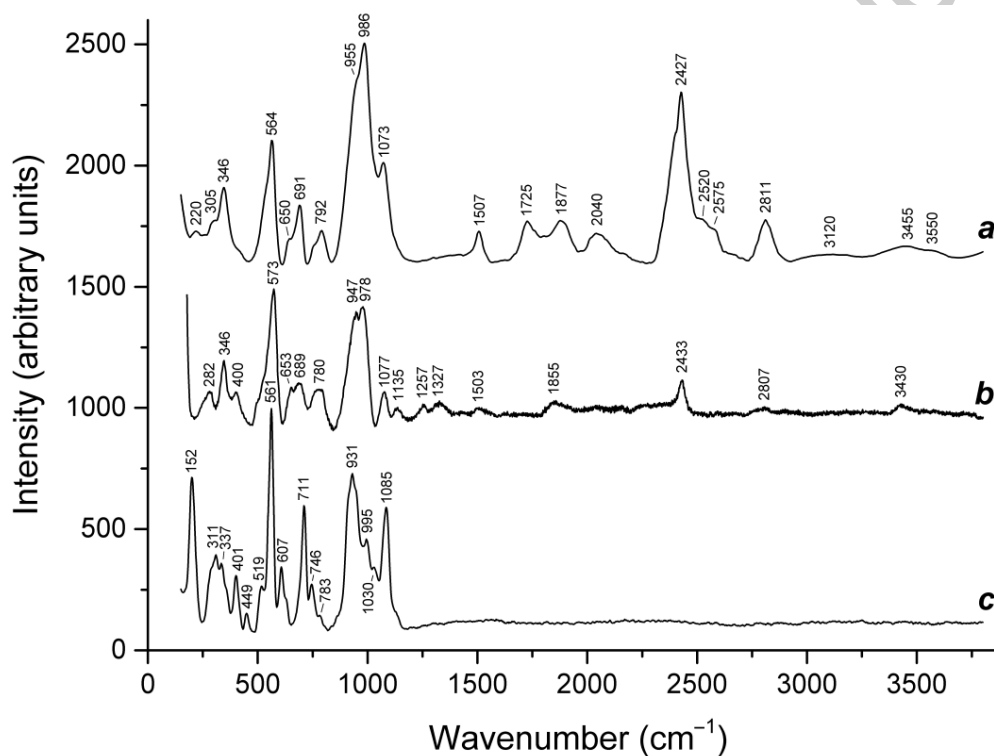


Fig. 3. Raman spectra of (a) selsurtite, (b) amableite-(Ce) and (c) eudialyte.

Chemical Data

Analytical data are given in Table 1. Contents of other elements with atomic numbers >8 are below detection limits.

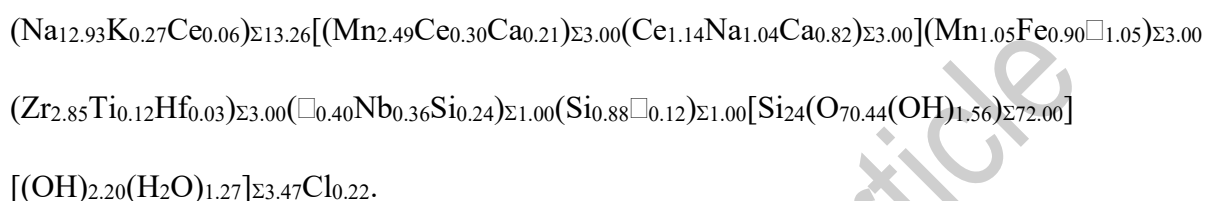
Based on IR spectroscopy data, all iron is considered as Fe^{3+} . It is to be noted that Fe^{3+} and Fe^{2+} cations at the $M2$ site of eudialyte-group minerals are yellow and red (to brownish-red in the

case of five-fold coordination) chromophores, respectively (Pol'shin *et al.*, 1991). Thus, yellow colour of amableite-(Ce) indicates the absence of Fe²⁺ at the M2 site.

Trivalent state of iron is also in agreement with a superior Gladstone-Dale compatibility index $CI = 1 - (K_p/K_c) = -0.014$ (Mandarino, 1981). To compare: with Fe²⁺, CI would be -0.026 .

The bulk empirical formula of amableite-(Ce) is $H_{5.76}Na_{14.00}K_{0.27}Ca_{1.03}Ce_{0.78}La_{0.58}Nd_{0.11}Pr_{0.03}Mn_{3.55}Fe_{0.92}Ti_{0.26}Zr_{2.77}Hf_{0.035}Nb_{0.35}Si_{25.12}Cl_{0.22}O_{75.36}$.

Based on the structural data (see below), it can be written as follows:



The simplified formula is $(Na,H,K,Ce)_{15}[(Ce,Na,Ca)_3(Mn,Ce,Ca)_3](Mn,Fe,\square)_3(Zr,Ti)_3$
 $(\square,Nb,Si)(Si,\square)Si_{24}(O,OH)_{72}[(OH,H_2O,O)_3]$, and the ideal formula is $Na_{15}[(Ce_{1.5}Na_{1.5})Mn_3]Mn_2Zr_3\square Si[Si_{24}O_{69}(OH)_3](OH)_2 \cdot H_2O$.

X-ray Diffraction and Crystal Structure

Powder X-ray diffraction data of amableite-(Ce) are given in Table 3. The unit-cell parameters refined from the powder data are: $a = 14.140(3)$ Å, $c = 30.37(1)$ Å, and $V = 5258(4)$ Å³.

The crystal structure of amableite-(Ce) (Figs. 4 and 5) was refined on the basis of 6462 independent reflections with $I > 2\sigma(I)$. The final refinement cycles converged to $R_1 = 4.23\%$,

The atomic coordinates occupancies, site-scattering values and equivalent isotropic parameters are given in Table 4. The anisotropic displacement parameters and selected bond lengths are given in Tables 5 and 6, respectively. See Discussion section for further details.

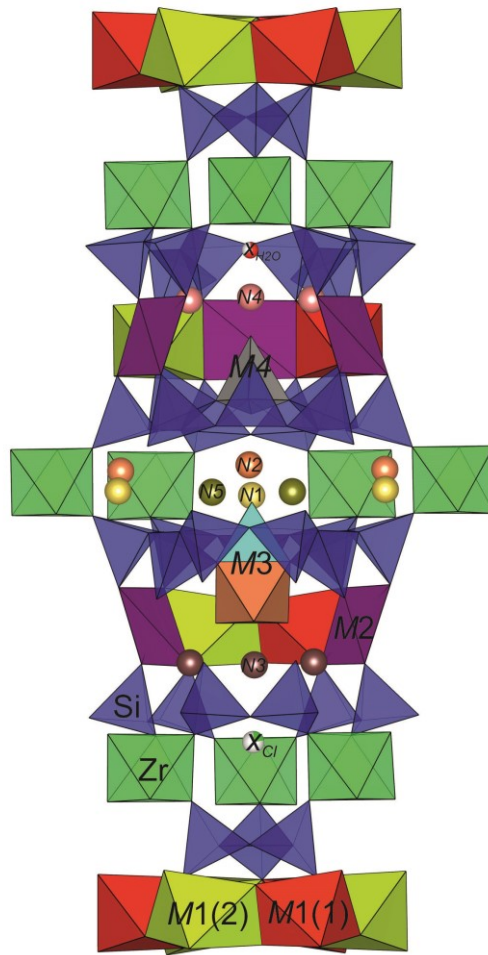


Fig. 4. The crystal structure of amableite-(Ce): general view.

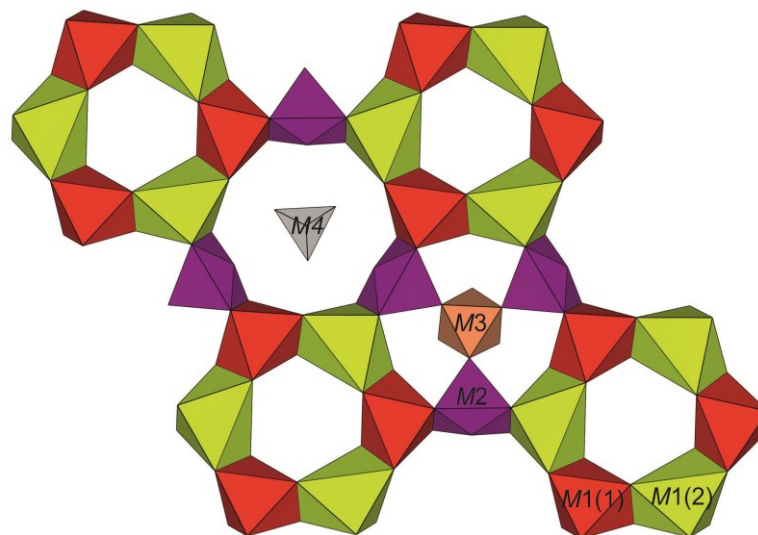


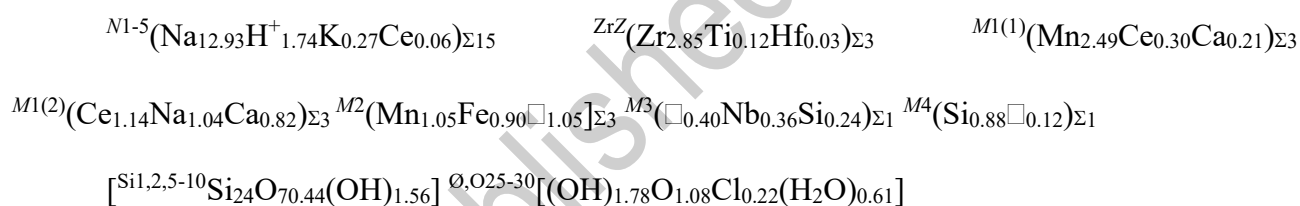
Fig. 5. A local arrangement involving 6-membered rings of octahedra in the structure of amableite-(Ce).

The crystallographic information file (cif) has been deposited *via* the joint Cambridge Crystallographic Data Centre CCDC/FIZ Karlsruhe deposition service <https://www.ccdc.cam.ac.uk/structures/> (the deposition number is CSD 2325823) and also are available as Supplementary Material.

Discussion

Crystal structure

Amableite-(Ce) is isostructural with other 12-layered members of the oneillite subgroup of the eudialyte group with the space group $R\bar{3}$. Based on the refined site-scattering factors, the crystal chemical formula of amableite-(Ce) can be written as follows ($Z = 3$):



where $[\text{Si}_{1,2,5-10}\text{Si}_{24}\text{O}_{70.44}(\text{OH})_{1.56}]$ are rings of tetrahedra.

The following combination of structural features of amableite-(Ce) distinguishes it from other eudialyte-group minerals:

- (i) Cation ordering within the six-membered ring of octahedra resulting in a lowering of symmetry (Figure 5). The six-membered ring is formed by $M1(1)\text{O}_6$ - and $M1(2)\text{O}_6$ -octahedra with different occupancies. The $M1(1)\text{O}_6$ -octahedron is predominantly occupied by manganese (2.49 *apfu*), while the $M1(2)\text{O}_6$ -octahedron is predominantly occupied by Na and *REE*, with subordinate Ca.
- (ii) The predominance of Mn^{2+} at the $M2$ site.
- (iii) The predominance of vacancies over NbO_6 octahedra and $\text{SiO}_3(\text{OH})$ tetrahedra at the $M3$ site.

(iv) The predominance of Si at the *M4* site.

Comparative data for amableite-(Ce) and related eudialyte-group minerals are given in Table 7.

Raman spectroscopy of hydronium and hydrated proton complexes

Numerous *ab initio* quantum-chemical calculations of hydronium and other hydrated proton complexes, including Zundel (H_5O_2^+) and Eigen ($\text{H}_3\text{O}^+\cdot 3\text{H}_2\text{O}$) cations have shown that these clusters are characterized by variable configurations and strong hydrogen bonds with the $\text{O}\cdots\text{O}$ distances in the range of 2.38 – 2.8 Å (Vyas, 1978; Komatsuzaki and Ohmine, 1994; Corongiu, 1995; Kim *et al.*, 2002; Sobolewski and Domcke, 2002a,b; Asmis *et al.*, 2003; Christie, 2004; Headrick *et al.*, 2004; Laria *et al.*, 2004; Asthagiri *et al.*, 2005; Ortega *et al.*, 2005; Paddison *et al.*, 2005; Vener and Librovich, 2009; Biswas *et al.*, 2017; Carpenter, 2020). Calculated wavenumbers of vibrational modes corresponding to the hydrated proton complexes are in the range of 1070 – 3000 cm^{-1} .

There is a negative correlation between the frequency of O–H stretching vibrations and $\text{O}\cdots\text{O}$ distance between O atom of OH group and O atom – acceptor of hydrogen bond (McClellan and Pimentel, 1960; see Figure 6). This correlation is nearly linear in the range of the $\text{O}\cdots\text{O}$ distances from 2.4 to 2.8 Å and significantly deviates from the linearity for weaker hydrogen bonds.

The following empirical correlations between O–H stretching frequencies in IR spectra of minerals and $\text{O}\cdots\text{O}$ and $\text{H}\cdots\text{O}$ distances (obtained from structural data) were established by E.

Libowitzky (1999):

$$\nu (\text{cm}^{-1}) = 3592 - 304 \cdot 10^9 \cdot \exp[-d(\text{O}\cdots\text{O})/0.1321] \quad (1)$$

$$\nu (\text{cm}^{-1}) = 3632 - 1.79 \cdot 10^6 \cdot \exp[-d(\text{H}\cdots\text{O})/0.2146] \quad (2)$$

A similar correlation was obtained by Novak (1974).

Actually, the equations (1) and (2) are a very rough approximation and have a restricted applicability. In particular, above 3500 cm^{-1} substantial deviations from the correlations (1) and (2) are common because O–H stretching frequencies depend not only on O \cdots O and H \cdots O distances, but also on the nature of cations coordinating O–H groups and H₂O molecules, as well as on the O–H \cdots O angle, and the influence of these factors becomes most evident in the case of weak hydrogen bonds. The equations (1) and (2) predict that maximum possible values of O–H stretching frequencies for minerals are 3592 and 3632 cm^{-1} , respectively, but in many minerals including for magnesium serpentines, brucite, kaolinite, amphiboles *etc.* observed frequencies are much higher and can exceed 3700 cm^{-1} . However, these correlations can be used for semiquantitative estimations, at least for relatively strong hydrogen bonds.

According to the equation (1), the Raman bands of amableite-(Ce) observed at 1815 , 2433 and 2807 cm^{-1} correspond to the O \cdots O distances of 2.51 , 2.56 and 2.61 \AA , respectively which is rather close to the distances of 2.50 , 2.58 and 2.59 \AA for O7 \cdots O30, O7 \cdots O27 and O24 \cdots O29 in strong hydrogen bonds O–H \cdots O in amableite-(Ce).

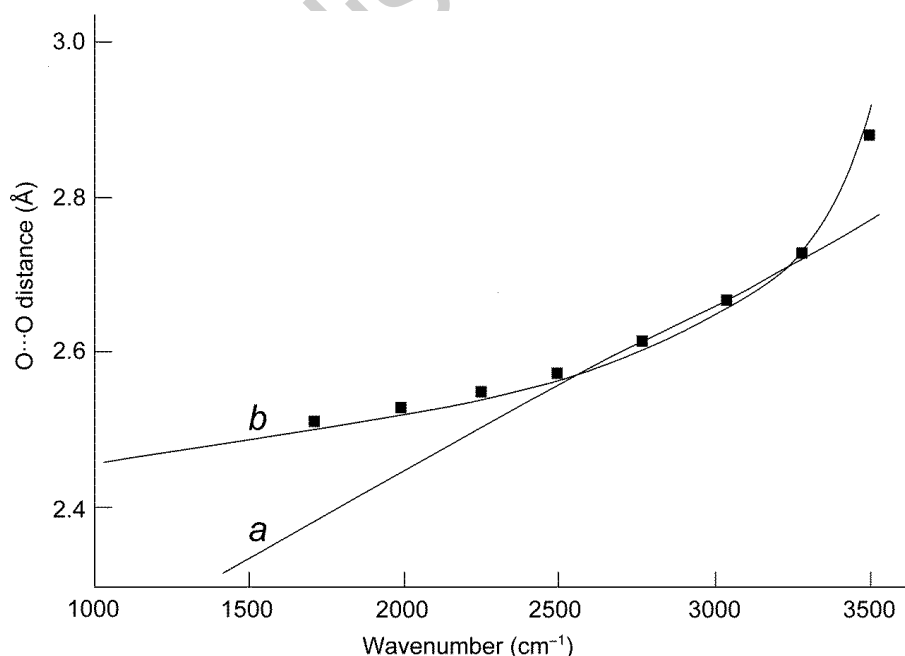


Fig. 6. The correlations between wavenumbers of O–H stretching vibrations and O \cdots O distances for hydrogen bonds in crystals drawn using data by McClellan and Pimentel (1960) (curve *a*), Libowitzky (1999) (curve *b*), and Novak (1974) (squares).

Implications

Minerals belonging to the eudialyte group are considered as potential sources of *REE*, Zr, Hf, Nb and Ta for industrial use (Lebedev, 2003; Lebedev *et al.*, 2003; Zakharov *et al.*, 2011; Friedrich *et al.*, 2016; Davis *et al.*, 2017; Ma *et al.*, 2019).

Almost all studied samples of EGMs contain detectable amounts of rare-earth elements (Rastsvetaeva *et al.*, 2012). Samples of EGMs from peralkaline pegmatites are characterized by the highest contents of these elements (typically, from 2 to 8 wt.% of REE_2O_3). Amableite-(Ce) is the third EGM after zirsilite-(Ce), $(Na, \square)_{12}(Ce, Na)_3Ca_6Mn_3Zr_3Nb(Si_{25}O_{73})(OH)_3(CO_3) \cdot H_2O$ (Khomyakov *et al.*, 2003) and johnsenite-(Ce), $Na_{12}(Ce, La, Sr, Ca)_3Ca_6Mn_3Zr_3W(Si_{25}O_{73})(OH, Cl)_2(CO_3)$ (Grice and Gault, 2006) containing *REE* as a species-defining component.

As a rule, *REE*-rich EGMs are enriched in Mn whereas *REE*-poor EGMs are enriched in Fe. This regularity may have a crystal-chemical origin and correspond to the situations where relatively small (Fe- and Ca-centered) or larger (Mn^{2+} and *REE*-centered) *M2*- and *M1*-octahedra share common edges. However, geochemical factors may also play a significant role.

Acknowledgements

The authors are grateful to Dr. Henric Friis and anonymous reviewers for useful comments. A part of this work, including chemical analyses, infrared spectroscopy, interpretation of the Raman spectra and identification of associated minerals was carried-out in accordance with the state task of Russian Federation, registration number 124013100858-3. The authors thank the X-ray Diffraction Centre of Saint-Petersburg State University for instrumental and computational resources.

Conflict of interest. The authors declare no conflict of interest.

Supplementary material. To view supplementary material for this article, please visit <https://www.ccdc.cam.ac.uk/structures/> (the deposition number is CSD 2325823).

Prepublished Article

References

- Asmis K.R., Pivonka N.L., Santambrogio G., Brümmer M., Kaposta C., Neumark D.M., Wöste L. (2003) The gasphase infrared spectrum of the protonated water dimer. *Science*, **299**, 1375–1381.
- Asthasgiri D., Pratt L.R., Kress J.D. (2005) *Ab initio* molecular dynamics and quasichemical study of $H^+(aq)$. *Proceedings of the National Academy of Sciences of the United States of America*, **102**, 6704–6708. www.pnas.org/cgi/doi/10.1073/pnas.0408071102
- Biswas R., Carpenter W., Fournier J.A., Voth G.A., Tokmakoff A. (2017) IR spectral assignments for the hydrated excess proton in liquid water. *Journal of Chemical Physics*, 146, paper 154507. <https://doi.org/10.1063/1.4980121>
- Britvin S.N., Dolivo-Dobrovolsky D.V., Krzhizhanovskaya M.G. (2017) Software for processing the X-ray powder diffraction data obtained from the curved image plate detector of Rigaku RAXIS Rapid II diffractometer. *Zapiski Rossiiskogo Mineralogicheskogo Obshchestva (Proc. Russ. Mineral. Soc.)*, **146(3)**, 104–107 (in Russian).
- Carpenter W.B. (2020) Aqueous proton structures and dynamics observed with nonlinear infrared spectroscopy. Ph. D. dissertation, the University of Chicago, 346 pp.
- Christie R.A. (2004) *Theoretical Studies of Hydrogen-Bonded Clusters*. Ph.D. Thesis, University of Pittsburgh, 135 pp.
- Chukanov N.V., Pekov I.V., Zadov A.E., Korovushkin V.V., Ekimenkova I.A., Rastsvetaeva R.K. (2003) Ikranite, $(Na,H_3O)_{15}(Ca,Mn,REE)_6Fe^{3+}_2Zr_3(\square,Zr)(\square,Si)Si_{24}O_{66}(O,OH)_6Cl \cdot nH_2O$, and raslakite, $Na_{15}Ca_3Fe_3(Na,Zr)_3Zr_3(Si,Nb)(Si_{25}O_{73})(OH,H_2O)_3(Cl,OH)$, new eudialyte-group minerals from the Lovizero massif. *Zapiski Rossiiskogo Mineralogicheskogo Obshchestva (Proceedings of the Russian Mineralogical Society)*, **132(5)**, 22–33 (in Russian).
- Chukanov N.V., Aksenov S.M., Pekov I.V., Belakovskiy D.I., Vozchikova S.A., Britvin S.N. (2020) Sergevanite, $Na_{15}(Ca_3Mn_3)(Na_2Fe)Zr_3Si_{26}O_{72}(OH)_3 \cdot H_2O$, a new eudialyte-group

- mineral from the Lovozero alkaline massif, Kola Peninsula. *The Canadian Mineralogist*, **58**, 421–436. DOI: 10.3749/canmin.2000006.
- Chukanov N.V., Vigasina M.F., Rastsvetaeva R.K., Aksenov S.M., Mikhailova Ju.A., Pekov I.V. (2022) The evidence of hydrated proton in eudialyte-group minerals based on Raman spectroscopy data. *Journal of Raman Spectroscopy*, **53**, 1188–1203. DOI: 10.1002/jrs.6343.
- Chukanov N.V., Aksenov S.M., Kazheva O.N., Pekov I.V., Varlamov D.A., Vigasina M.F., Belakovskiy D.I., Vozchikova S.A., Britvin S.N. (2023) Selsurtite, $(\text{H}_3\text{O})_{12}\text{Na}_3(\text{Ca}_3\text{Mn}_3)(\text{Na}_2\text{Fe})\text{Zr}_3\text{Si}[\text{Si}_{24}\text{O}_{69}(\text{OH})_3](\text{OH})\text{Cl}\cdot\text{H}_2\text{O}$, a new eudialyte-group mineral from the Lovozero alkaline massif, Kola Peninsula. *Mineralogical Magazine*, **87(2)**, 241–251. DOI: 10.1180/mgm.2022.136.
- Corongiu G., Kelterbaum R., Kochanski E. (1995) Theoretical Studies of $\text{H}^+(\text{H}_2\text{O})_5$. *Journal of Physical Chemistry*, **99**, 8038–8044. DOI: 10.1021/J100020A029.
- CrysAlisPro (2015) CrysAlisPro Software System, version 1.171.39.44. Rigaku Oxford Diffraction: Oxford, UK.
- Dolomanov O.V., Bourhis L.J., Gildea R.J., Howard J.A.K., Puschmann H. (2009) OLEX2: a complete structure solution, refinement and analysis program. *Journal of Applied Crystallography*, **42**, 339–341.
- Davis P., Stopic S., Balomenos E., Pantias D., Paspaliaris I., Friedrich B. (2017) Leaching of rare earth elements from eudialyte concentrate by suppressing silica gel formation. *Minerals Engineering*, **108**, 115–122.
- Dolomanov O.V., Bourhis L.J., Gildea R.J., Howard J.A.K., Puschmann H. (2009) OLEX2: a complete structure solution, refinement and analysis program. *Journal of Applied Crystallography*, **42**, 339–341.
- Friedrich B., Hanebuth M., Kruse S., Tremel A., Vossenkaul D. (2016) Method for opening a eudialyte mineral. Patent number EP2995692 A1.

- Grice J.D. and Gault R.A. (2006) Johnsenite-(Ce): a new member of the eudialyte group from Mont Saint-Hilaire, Quebec, Canada. *The Canadian Mineralogist*, **44**, 105–115.
- Headrick J.M., Bopp J.C., Johnson M.A. (2004) Predissociation spectroscopy of the argon-solvated H_5O_2^+ “Zundel” cation in the 1000 – 1900 cm^{-1} region. *Journal of Chemical Physics*, **121**, 11523–11526.
- Horváth L., Pfenninger Horváth E., Gault R.A., Tarasoff P. (1998) Mineralogy of the Saint Amable sill, Varennes and Saint Amable, Québec, Canada. *Mineralogical Record*, **29**, 83–118.
- Johnsen O., Grice J.D., Gault R.A. (1999) Oneillite: a new Ca-deficient and REE-rich member of the eudialyte group from Mont Saint-Hilaire, Québec, Canada. *The Canadian Mineralogist*, **37**, 1295–1301.
- Johnsen O., Ferraris G., Gault R.A., Grice J.D., Kampf A.R., Pekov I.V. (2003) Nomenclature of eudialyte-group minerals. *The Canadian Mineralogist*, **41**, 785–794.
- Kohmyakov A.P., Dusmatov V.D., Ferraris G., Gula A., Ivaldi G., Nechelyustov G.N. (2003) Zirsilite-(Ce), $((\text{Na}, \square)_{12}(\text{Ce}, \text{Na})_3\text{Ca}_6\text{Mn}_3\text{Zr}_3\text{Nb}(\text{Si}_{25}\text{O}_{73})(\text{OH})_3(\text{CO}_3)\cdot\text{H}_2\text{O}$, and carbokentbrooksit, $((\text{Na}, \square)_{12}(\text{Na}, \text{Ce})_3\text{Ca}_6\text{Mn}_3\text{Zr}_3\text{Nb}(\text{Si}_{25}\text{O}_{73})(\text{OH})_3(\text{CO}_3)\cdot\text{H}_2\text{O}$ – two new eudialyte-group minerals from the Dara-i-Pioz alkaline massif, Tajikistan. *Zapiski Rossiiskogo Mineralogicheskogo Obshchestva (Proceedings of the Russian Mineralogical Society)*, **132(5)**, 40–51 (in Russian).
- Khomyakov A.P., Nechelyustov G.N., Rastsvetaeva, R.K. (2007) Aqualite, $(\text{H}_3\text{O})_8(\text{Na}, \text{K}, \text{Sr})_5\text{Ca}_6\text{Zr}_3\text{Si}_{26}\text{O}_{66}(\text{OH})_9\text{Cl}$, a new eudialyte-group mineral from Inagli alkaline massif (Sakha-Yakutia, Russia), and the problem of oxonium in hydrated eudialytes. *Zapiski Rossiiskogo Mineralogicheskogo Obshchestva (Proceedings of the Russian Mineralogical Society)*, **136(2)**, 39–55 (in Russian).
- Khomyakov A.P., Nechelyustov G.N., Rastsvetaeva R.K. (2009) Voronkovite, $\text{Na}_{15}(\text{Na}, \text{Ca}, \text{Ce})_3(\text{Mn}, \text{Ca})_3\text{Fe}_3\text{Zr}_3\text{Si}_{26}\text{O}_{72}(\text{OH}, \text{O})_4\text{Cl}\cdot\text{H}_2\text{O}$, a new mineral species of the

- eudialyte group from the Lovozero alkaline pluton, Kola Peninsula, Russia. *Geology of Ore Deposits*, **51(8)**, 750–756.
- Kim J., Schmitt U.W., Gruetzmacher J.A., Voth G.A., Scherer N.E. (2002) The vibrational spectrum of the hydrated proton: Comparison of experiment, simulation, and normal mode analysis. *Journal of Chemical Physics*, **116**, 737–746.
- Komatsuzaki T. and Ohmine I. (1994) Energetics of proton transfer in liquid water. I. Ab initio study for origin of many-body interaction and potential energy surfaces. *Chemical Physics*, **180**, 239–269. DOI: 10.1016/0301-0104(93)e0424-t.
- Laria D., Martí J., Guàrdia E. (2004) Protons in supercritical water: A multistage empirical valence bond study. *Journal of American Chemical Society*, **126**, 2125–2134. DOI: 10.1021/ja0373418.
- Lebedev V.N. (2003) Sulfuric acid technology for processing of eudialyte concentrate. *Russian Journal of Applied Chemistry*, **76(10)**, 1559–1563.
- Lebedev V.N., Shchur T.E., Maiorov D.V., Popova L.A., Serkova R.P. (2003) Specific features of acid decomposition of eudialyte and certain rare-metal concentrates from Kola Peninsula. *Russian Journal of Applied Chemistry*, **76(8)**, 1191–1196.
- Libowitzky E. (1999) Correlation of O–H stretching frequencies and O–H···O hydrogen bond lengths in minerals. *Monatshefte für Chemie*, **130**, 1047–1059.
- McClellan A.L. and Pimentel G.C. (1960) Hydrogen bond. W.H.Freeman & Co Ltd, California Univ. 475 pp.
- Novak A. (1974) Hydrogen bonding in solids correlation of spectroscopic and crystallographic data. In: *Large Molecules*, Springer, Berlin-Heidelberg, 177–216. DOI: 10.1007/BFb0116438.
- Ma Y.Q., Stopic, S. Huang Z.Z., Freidrich B. (2019) Selective recovery and separation of Zr and Hf from sulfuric acid leach solution using anion exchange resin. *Hydrometallurgy*, **189**, UNSP 105143.

- Mandarino J.A. (1981) The Gladstone-Dale relationship. IV. The compatibility concept and its application. *The Canadian Mineralogist*, **41**, 989–1002.
- Ortega I.K., Escribano R., Herrero V.J., Maté B., Moreno M.A. (2005) The structure and vibration frequencies of crystalline HCl trihydrate. *Journal of Molecular Structure*, **742**, 147–152. DOI: 10.1016/j.molstruc.2005.01.005.
- Paddison S.J. and Elliott J.A. (2005) Molecular modeling of the short-side-chain perfluorosulfonic acid membrane. *Journal of Physical Chemistry A*, **109**, 7583–7593, <https://doi.org/10.1021/jp0524734>
- Pol'shin E.V., Platonov A.N., Borutsky B.E., Taran M.N., Rastsvetaeva R.K. (1991) Optical and Mössbauer Study of Minerals of the Eudialyte Group. *Physics and Chemistry of Minerals*, **18**, 117–125.
- Rastsvetaeva, R.K., Chukanov, N.V., Aksenov, S.M. (2012) Eudialyte-Group Minerals. Nizhny Novgorod State University, Nizhny Novgorod. 230 pp. (in Russian).
- Sheldrick G.M. (2015) Crystal structure refinement with SHELXL. *Acta Crystallographica*, **C71**, 3–8.
- Shtuckenberg A. and Punin Yu.O.B. (2007) *Optically anomalous crystals*. Dordrecht, the Netherlands: Springer, 279 pp.
- Sobolewski A.L. and Domcke W. (2002a) Hydrated hydronium: a cluster model or solvated electron? *Physical Chemistry Chemical Physics*, **4**, 4–10. DOI: 10.1039/b107373g.
- Sobolewski A.L. and Domcke W. (2002b) *Ab initio* investigation of the structure and spectroscopy of hydronium-water clusters. *Journal of Physical Chemistry A*, **106**, 4158–4167.
- STOE (2003) WinXPow Version 2.08, STOE & Cie GmbH, Darmstadt, Germany.
- Vener M.V. and Librovich N.B. (2009) The structure and vibrational spectra of proton hydrates: H_5O_2^+ as a simplest stable ion. *International Reviews in Physical Chemistry*, **28**, 407–434. DOI: 10.1080/01442350903079955.

Vyas N.K., Sakore T.D., Biswas A.B. (1978) The structure of 4-methyl-5-sulphosalicylic acid tetrahydrate. *Acta Crystallographica B*, **34**, 3486–3488.

<https://doi.org/10.1107/S0567740878011413>

Zakharov V.I., Maiorov D.V., Alishkin A.R., Matveev V.A. (2011) Causes of insufficient recovery of zirconium during acidic processing of Lovosero eudialyte concentrate. *Russian Journal of Non-Ferrous Metals*, **52(5)**, 423–428.

Prepublished Article

List of Figures:

FIG. 1. Amableite-(Ce) crystals (yellow) in association with albite, aegirine and natrolite. FOV width is 3.5 mm. Photographer: V. Heck.

FIG. 2. Powder infrared absorption spectra of (a) amableite-(Ce) and (b) holotype sample of voronkovite (Khomyakov *et al.*, 2009), an oneillite-type EGM related to amableite-(Ce). The spectra are offset for comparison.

FIG. 3. Raman spectra of (a) selsurtite, (b) amableite-(Ce) and (c) eudialyte.

FIG. 4. The crystal structure of amableite-(Ce): general view.

FIG. 5. A local situation involving 6-membered rings of octahedra in the amableite-(Ce) structure.

FIG. 6. The correlations between wavenumbers of O–H stretching vibrations and O···O distances for hydrogen bonds in crystals drawn using data by McClellan and Pimentel (1960) (curve a), Libowitzky (1999) (curve b), and Novak (1974) (squares).

Prepublished Article

Table 1. Crystal data, data collection information and structure refinement details for amableite-(Ce).

Crystal system	Trigonal
Space group	$R\bar{3}$
a , Å	14.1340(3)
c , Å	30.3780(11)
V , Å ³	5255.6(3)
Z	3
μ , mm ⁻¹	2.912
$F(000)$	4398.0
Crystal size, mm ³	0.18 × 0.12 × 0.09
Temperature, K	293(2)
Radiation	Mo K α ($\lambda = 0.71073$)
2 Θ range for data collection, °	6.792 to 67.286
Index ranges	$-19 \leq h \leq 21$, $-21 \leq k \leq 21$, $-41 \leq l \leq 45$
Reflections collected	12263
Independent reflections	6914 ($R_{\text{int}} = 0.0214$, $R_{\text{sigma}} = 0.0318$)
Data/restraints/parameters	6914/3/449
Goodness-of-fit on F^2	1.035
Final R indexes [$I > 2\sigma(I)$]	$R_1 = 0.0423$, $wR_2 = 0.1120$
Final R indexes [all data]	$R_1 = 0.0450$, $wR_2 = 0.1138$
Largest diff. peak/hole, e \cdot Å ⁻³	1.31/-1.65
Flack parameter	0.16(2)

Table 2. Chemical composition of amableite-(Ce).

Constituent	Content, wt. %	Range	Standard deviation	Standard
Na ₂ O	14.20	13.75 – 14.56	0.26	Albite
K ₂ O	0.41	0.29 – 0.48	0.07	Orthoclase
CaO	1.89	1.79 – 1.98	0.06	Wollastonite
MnO*	8.25	8.02 – 8.50	0.12	Mn
Fe ₂ O ₃	2.40	2.07 – 2.85	0.21	Fe
La ₂ O ₃	3.10	2.93 – 3.25	0.10	LaPO ₄
Ce ₂ O ₃	4.19	3.98 – 4.34	0.12	CePO ₄
Pr ₂ O ₃	0.16	0 – 0.25	0.08	PrPO ₄
Nd ₂ O ₃	0.59	0.50 – 0.69	0.07	NdPO ₄
SiO ₂	49.41	49.16 – 49.87	0.25	SiO ₂
ZrO ₂	11.17	11.09 – 11.44	0.13	Zr
HfO ₂	0.24	0.18 – 0.29	0.04	Hf
TiO ₂	0.68	0.54 – 0.81	0.08	Ti
Nb ₂ O ₅	1.54	1.30 – 1.67	0.12	Nb
Cl	0.26	0.21 – 0.30	0.03	NaCl
H ₂ O**	1.70			
–O≡Cl	–0.06			
Total	100.13			

*Bivalent state of Mn and trivalent state of Fe are in agreement with the IR spectrum (see above) and structural data. In addition, Mn³⁺ is a very strong purple chromophore whereas amableite-(Ce) is yellow.

**The content of H₂O was determined by means of a modified Penfield method.

Table 3. Powder X-ray diffraction data (d in Å) of amableite-(Ce).

I_{obs} , %	d_{obs} , Å	I_{calc} , %*	d_{calc} , Å**	hkl
51	11.34	57	11.353	101
11	10.11	5	10.126	003
13	9.53	19	9.531	012
76	7.06	89	7.067	110
20	6.45	29	6.453	104
32	6.00	21	6.000	021
27	5.67	24	5.677	202
13	5.44	16	5.442	015
2	5.07	2	5.063	006
4	4.422	2	4.426	-132
63	4.312	64	4.312	205
22	4.100	16, 6, 7	4.116, 4.090, 4.080	116, 107, 300
26	3.951	25	3.951	214
38	3.783	36	3.784	033
8	3.678	6	3.681	125
6	3.627	7	3.627	018
43	3.538	33, 11	3.540, 3.534	027, 220
31	3.373	23	3.374	-141
19	3.326	12, 10	3.336, 3.313	223, 312
20	3.224	19	3.227	208
30	3.168	9, 22	3.177, 3.165	036, -237
21	3.044	19, 1	3.046, 3.045	119, 401
13	2.998	8	3.000	042
84	2.963	80	2.964	-345
14	2.898	12	2.898	226
100	2.837	100	2.838	404
3	2.796	2	2.796	-351
5	2.760	2	2.761	-252
10	2.721	11	2.721	0.2.10
22	2.674	20, 6	2.674, 2.671	137, 140
19	2.633	19	2.634	-354
17	2.600	26	2.601	039
9	2.532	8, 2	2.536, 2.531	0.0.12, -348
14	2.441	8, 9	2.441, 2.440	229, 051
11	2.382	11	2.383	048
8	2.362	6	2.362	-456
11	2.306	13	2.307	-261
5	2.260	2, 3	2.264, 2.258	-1.4.10, -258
3	2.193	1	2.193	-561
8	2.176	5	2.176	-162
28	2.157	8, 23	2.162, 2.156	-465, 4.0.10
13	2.140	8, 4, 2	2.142, 2.137, 2.136	-3.4.11, 0.1.14, -366
8	2.112	7	2.112	514
6	2.095	4	2.095	-159

8	2.062	2, 5, 2	2.067, 2.062, 2.058	155, -3.5.10, 2.2.12
4	2.043	1, 2	2.045, 2.041	2.0.14, 247
5	2.009	5	2.008	431
5	2.001	3	2.000	603
11	1.975	11, 2	1.976, 1.969	428, -2.5.11
5	1.962	2, 1, 1	1.965, 1.961, 1.960	-1.3.14, -567, 520
4	1.945	2, 2	1.947, 1.945	1.1.15, -474
5	1.930	4, 2, 1	1.932, 1.925, 1.924	-369, 1.3.13, -273
2	1.909	1, 1	1.910, 1.906	-375, 0.5.10
7	1.892	7	1.892	606
3	1.863	4	1.863	-171
3	1.854	3	1.853	612
7	1.837	3, 5	1.840, 1.837	-2.6.10, 4.1.12
9	1.829	8, 3	1.829, 1.826	256, 437
2	1.813	1, 1	1.813, 1.813	0.2.16, -174
10	1.781	1, 6	1.784, 1.781	615, 5.1.10
24	1.769	10, 10, 18	1.773, 1.770, 1.767	-4.6.11, 0.4.14, 440
6	1.747	1, 6	1.746, 1.746	069, 701
2	1.726	2	1.725	-3.6.12
5	1.716	5, 2	1.717, 1.715	-2.5.14, 2.0.17
3	1.696	4	1.695	621
6	1.688	1, 7	1.688, 1.687	0.0.18, -282
9	1.668	12	1.668	446
5	1.643	5, 3	1.644, 1.642	2.4.13, 1.1.18
8	1.637	9	1.635	265
10	1.613	3, 13	1.614, 1.613	1.4.15, 4.0.16
2	1.602	3	1.601	-783
5	1.590	4	1.590	-1.7.10
7	1.581	1, 1, 7	1.583, 1.581, 1.581	-4.6.14, 3.1.17, 627
5	1.573	7	1.573	3.2.16
2	1.559	1, 1	1.560, 1.559	0.3.18, 452
4	1.550	3	1.550	2.5.12
7	1.544	6	1.544	1.5.14
6	1.524	4, 1, 1, 4	1.525, 1.525, 1.523, 1.522	4.3.13, -693, 2.2.18, 802
2	1.500	2, 1	1.500, 1.500	0.5.16, 084
7	1.478	2, 8	1.482, 1.477	6.2.10, 0.7.11
2	1.468	3, 1	1.468, 1.467	2.4.16, -294
4	1.446	1, 1, 3	1.446, 1.446, 1.443	-1.4.19, -2.8.11, -1.3.20
2	1.439	2	1.437	0.6.15
3	1.420	3	1.419	808

*For the calculated pattern, only reflections with intensities ≥ 1 are given.

**For the unit-cell parameters calculated from single-crystal data.

Table 4. Atomic coordinates, occupancies, site-scattering values and equivalent isotropic displacement parameters (\AA^2) for amableite-(Ce).

Site	x	y	z	Occupancy	s.s. calc*	s.s.*	U(eq)
ZrZ	0.33321(6)	0.16067(5)	0.43713(3)	Zr _{0.95} Ti _{0.04} Hf _{0.01}	39.60	40.0	0.0149(1)
<i>M1(1)</i>							
Mn1	0.3938(4)	0.0606(4)	0.6038(1)	Mn _{0.83} Ce _{0.10} Ca _{0.07}	27.95	22.25	0.0152(6)
Mn1A	0.424(1)	0.090(1)	0.6041(2)			5.50	0.011(2)
<i>M1(2)</i>							
Ce1_2	0.4242(4)	0.3336(1)	0.60390(6)	Ce _{0.38} Na _{0.35} Ca _{0.27}	31.29	24.36	0.0171(7)
Na1_2	0.394(2)	0.3316(9)	0.6034(4)			6.50	0.029(3)
<i>M2</i>							
Mn2_1	0.4943(8)	0.4934(8)	0.2705(2)	Mn _{0.35} □ _{0.35} Fe _{0.30}	16.55	12.75	0.049(7)
Mn2_2	0.469(2)	0.525(2)	0.2718(9)			2.00	0.021(6)
Mn2_3	0.523(2)	0.473(2)	0.2682(9)			1.63	0.014(7)
Si1	0.3927(1)	0.3814(1)	0.36682(7)	Si	14.0	14.0	0.0172(4)
Si2	0.6079(1)	0.6001(1)	0.36659(7)	Si	14.0	14.0	0.0167(4)
Si5	0.2740(1)	0.3221(1)	0.50743(7)	Si	14.0	14.0	0.0171(4)
Si6	0.2071(1)	0.4149(2)	0.34589(8)	Si	14.0	14.0	0.0211(4)
Si7	0.5263(1)	0.2521(2)	0.52327(8)	Si	14.0	14.0	0.0205(4)
Si8	0.0586(1)	0.3253(1)	0.50773(7)	Si	14.0	14.0	0.0163(4)
Si9	0.5856(2)	0.1928(1)	0.68446(7)	Si	14.0	14.0	0.0199(4)
Si10	0.4597(2)	0.5413(2)	0.52849(8)	Si	14.0	14.0	0.0217(4)
<i>M3</i>							
NbM3	1/3	2/3	0.5585(2)	□ _{0.40} Nb _{0.36} Si _{0.24}	17.85	14.35	0.047(2)
SiM3	1/3	2/3	0.5152(8)			3.50	0.039(8)
<i>M4</i>							
SiM4	1/3	2/3	0.3167(2)	Si _{0.88} □ _{0.12}	12.32	10.22	0.030(2)
SiM4A	1/3	2/3	0.3594(9)			2.10	0.016(8)
<i>N1-N5</i>							
NaN1	0.5514(4)	0.4416(4)	0.4499(2)	Na	11.0	11.0	0.052(1)
NaN2	0.1169(5)	0.2285(6)	0.4225(2)	Na	11.0	6.60	0.027(1)
NaN2A	0.086(2)	0.167(2)	0.4389(6)			4.40	0.11(1)
NaN3	0.4612(5)	0.2283(4)	0.3151(2)	Na _{0.89} K _{0.09} Ce _{0.02}	12.66	11.83	0.058(2)
NaN3A	0.528(4)	0.263(3)	0.324(2)			1.59	0.06(1)
NaN4	0.2034(7)	0.0996(4)	0.5593(4)	Na _{0.71} H ⁺ _{0.29}	7.81	7.15	0.031(3)
NaN4A	0.187(4)	0.093(4)	0.580(3)			0.66	0.01(2)
NaN5	0.268(2)	0.533(1)	0.4492(5)	Na _{0.71} H ⁺ _{0.29}	7.81	7.81	0.153(9)

O1	0.2666(6)	0.2903(6)	0.5577(3)	O	8.0	8.0	0.041(2)
O2	0.3932(4)	0.4304(5)	0.4975(2)	O	8.0	8.0	0.029(1)
O3	0.4073(6)	0.3024(6)	0.3996(3)	O	8.0	8.0	0.036(2)
O4	0.4850(4)	0.5067(4)	0.3805(3)	O	8.0	8.0	0.030(1)
O5	0.2609(5)	0.2282(5)	0.4748(3)	O	8.0	8.0	0.033(1)
O6	0.7192(5)	0.2620(5)	0.6810(3)	O	8.0	8.0	0.033(1)
O7	0.3883(7)	0.5991(6)	0.5313(4)	O	8.0	8.0	0.054(2)
O8	0.4009(5)	0.3591(6)	0.3161(2)	O	8.0	8.0	0.035(1)
O9	0.4953(5)	0.5169(5)	0.5750(3)	O	8.0	8.0	0.031(1)
O10	0.2736(5)	0.3716(5)	0.3759(2)	O	8.0	8.0	0.028(1)
O11	0.6884(5)	0.5862(5)	0.3988(3)	O	8.0	8.0	0.035(1)
O12	-0.0223(5)	0.2293(5)	0.4757(3)	O	8.0	8.0	0.031(1)
O13	0.1813(5)	0.3543(5)	0.4939(3)	O	8.0	8.0	0.030(1)
O14	0.1731(6)	0.3575(6)	0.2993(3)	O	8.0	8.0	0.030(1)
O15	0.5959(5)	0.3858(5)	0.5261(3)	O	8.0	8.0	0.033(2)
O16	0.5525(6)	0.1366(6)	0.7315(3)	O	8.0	8.0	0.041(2)
O17	0.4714(6)	0.2217(7)	0.4754(3)	O	8.0	8.0	0.040(2)
O18	0.0510(6)	0.4347(5)	0.4971(2)	O	8.0	8.0	0.033(1)
O19	0.0369(6)	0.2968(6)	0.5591(2)	O	8.0	8.0	0.035(1)
O20	0.5359(6)	0.1122(5)	0.6438(2)	O	8.0	8.0	0.039(1)
O21	0.4452(5)	0.2037(6)	0.5639(2)	O	8.0	8.0	0.039(1)
O22	0.6282(6)	0.5914(5)	0.3148(2)	O	8.0	8.0	0.029(1)
O23	0.1012(5)	0.3849(6)	0.3767(2)	O	8.0	8.0	0.031(1)
O24	0.2787(7)	0.5449(5)	0.3432(4)	O	8.0	8.0	0.059(3)
<i>O, OH, Cl, H₂O</i>							
O25	0	0	0.5028(8)	(H ₂ O) _{0.61}	4.88	4.88	0.050**
O26	1/3	2/3	0.268(1)	OH _{0.73}	5.84	5.84	0.12(1)
O27	0.277(2)	0.731(2)	0.6012(7)	O _{0.36} OH _{0.22}	4.64	4.72	0.089(9)
Cl28	2/3	1/3	0.407(1)	Cl _{0.22}	3.74	3.74	0.050**
O29	1/3	2/3	0.413(1)	OH _{0.15}	1.20	1.20	0.050**
O30	1/3	2/3	0.461(1)	OH _{0.24}	1.92	1.92	0.050**

*s.s. – site scattering and calc. s.s. – calculated site scattering (e.p.f.u).

** Fixed parameters.

Table 5. Anisotropic displacement parameters (\AA^2) for amableite-(Ce).

Site	U_{11}	U_{22}	U_{33}	U_{23}	U_{13}	U_{12}
ZrZ	0.0142(2)	0.0157(3)	0.0144(2)	0.0003(2)	0.0007(2)	0.0071(2)
Mn1	0.015(1)	0.015(1)	0.0136(6)	0.001(5)	-0.0011(5)	0.006(1)
Ce1_2	0.020(1)	0.0097(6)	0.0172(6)	-0.0011(3)	-0.0002(5)	0.0038(5)
Na1_2	0.014(5)	0.040(6)	0.032(5)	0.002(3)	-0.003(3)	0.013(4)
Mn2	0.039(5)	0.040(5)	0.018(2)	0.012(2)	-0.011(2)	-0.017(5)
Si1	0.0130(7)	0.0190(8)	0.019(1)	0.0023(7)	-0.0004(6)	0.0076(6)
Si2	0.0203(8)	0.0133(7)	0.016(1)	0.0018(6)	0(7)	0.0083(6)
Si5	0.0127(7)	0.0162(8)	0.019(1)	-0.0024(7)	-0.0005(6)	0.0050(6)
Si6	0.0164(8)	0.0213(9)	0.027(1)	-0.0079(8)	-0.0024(7)	0.0107(7)
Si7	0.0095(7)	0.0279(9)	0.018(1)	-0.0006(7)	0.0015(6)	0.0050(6)
Si8	0.0198(8)	0.0178(8)	0.015(1)	-0.0020(6)	-0.0002(6)	0.0123(6)
Si9	0.0279(9)	0.0088(7)	0.0161(9)	-0.0022(6)	-0.0008(7)	0.0041(6)
Si10	0.0163(8)	0.0161(8)	0.029(1)	0.0049(7)	-0.0029(7)	0.0056(7)
NbM3	0.039(2)	0.039(2)	0.064(4)	0	0	0.019(1)
SiM3	0.035(8)	0.035(8)	0.05(2)	0	0	0.017(4)
SiM4	0.023(2)	0.023(2)	0.043(4)	0	0	0.012(1)
SiM4A	0.008(7)	0.008(7)	0.03(2)	0	0	0.004(4)
NaN1	0.042(2)	0.055(3)	0.039(3)	0.012(2)	-0.013(2)	0.009(2)
NaN2	0.021(2)	0.037(3)	0.020(3)	-0.006(2)	-0.006(2)	0.012(2)
NaN2A	0.10(1)	0.24(3)	0.07(1)	-0.10(2)	-0.06(1)	0.14(2)
NaN3	0.079(4)	0.038(2)	0.071(4)	-0.019(2)	-0.034(3)	0.041(2)
NaN4	0.052(4)	0.013(2)	0.037(6)	-0.011(2)	-0.022(4)	0.024(2)
NaN5	0.23(2)	0.12(1)	0.12(1)	-0.020(8)	-0.02(1)	0.09(1)
O1	0.037(3)	0.041(4)	0.022(4)	0.002(3)	-0.004(3)	0.004(3)
O2	0.015(2)	0.022(2)	0.040(4)	-0.006(2)	0(2)	0.0007(2)
O3	0.034(3)	0.034(3)	0.043(4)	0.022(3)	0.010(3)	0.020(3)
O4	0.020(2)	0.019(2)	0.044(5)	-0.002(2)	0.002(2)	0.004(2)
O5	0.035(3)	0.027(3)	0.037(4)	-0.011(3)	0.002(3)	0.017(3)
O6	0.023(2)	0.024(2)	0.058(4)	0.005(2)	0.006(2)	0.016(2)
O7	0.048(4)	0.040(4)	0.089(7)	-0.003(4)	-0.008(4)	0.034(4)
O8	0.034(3)	0.057(4)	0.022(3)	-0.010(3)	-0.005(2)	0.028(3)
O9	0.037(3)	0.031(3)	0.023(4)	0.007(2)	-0.001(2)	0.015(3)
O10	0.018(2)	0.029(3)	0.037(4)	0(2)	0.002(2)	0.013(2)
O11	0.029(3)	0.033(3)	0.043(4)	-0.005(3)	-0.019(3)	0.016(3)
O12	0.031(3)	0.025(3)	0.036(4)	-0.008(3)	-0.010(3)	0.012(2)
O13	0.022(2)	0.032(3)	0.039(4)	0.002(2)	0.002(2)	0.016(2)

O14	0.041(3)	0.031(3)	0.019(3)	-0.006(3)	0(2)	0.019(3)
O15	0.023(2)	0.019(2)	0.064(5)	-0.006(3)	-0.003(3)	0.015(2)
O16	0.047(4)	0.034(3)	0.029(4)	0.010(3)	0.005(3)	0.010(3)
O17	0.028(3)	0.060(4)	0.021(3)	-0.010(3)	-0.007(2)	0.015(3)
O18	0.059(4)	0.029(3)	0.028(3)	0.001(2)	0.003(3)	0.034(3)
O19	0.060(4)	0.034(3)	0.020(3)	0.002(2)	0.006(3)	0.030(3)
O20	0.052(4)	0.033(3)	0.031(3)	-0.019(3)	-0.011(3)	0.022(3)
O21	0.035(3)	0.051(4)	0.026(3)	0.014(3)	0.018(3)	0.017(3)
O22	0.047(3)	0.027(3)	0.019(3)	0.006(2)	0.007(2)	0.022(3)
O23	0.026(3)	0.053(4)	0.025(3)	-0.003(3)	-0.005(2)	0.028(3)
O24	0.045(4)	0.013(3)	0.115(9)	0.001(4)	-0.007(5)	0.011(3)

Prepublished Article

Table 6. Selected bond lengths d (Å) in amableite-(Ce).

Atom	Atom	d		Atom	Atom	d		Atom	Atom	d
ZrZ	O3	2.076(7)		Si1	O3	1.585(7)		NaN1	O2	2.601(9)
ZrZ	O5	2.059(7)		Si1	O4	1.643(6)		NaN1	O3	2.520(10)
ZrZ	O11	2.068(6)		Si1	O8	1.590(8)		NaN1	O4	2.652(9)
ZrZ	O12	2.067(7)		Si1	O10	1.641(6)		NaN1	O11	2.526(9)
ZrZ	O16	2.051(7)		<Si1	O>	1.615		NaN1	O15	2.620(9)
ZrZ	O17	2.056(7)						NaN1	O17	2.833(10)
<ZrZ	O>	2.063		Si2	O4	1.628(6)		NaN1	O17	2.559(9)
				Si2	O11	1.588(7)		NaN1	O18	2.775(10)
Mn1	O9	2.274(7)		Si2	O22	1.613(7)		NaN1	Cl28	3.036(12)
Mn1	O14	2.292(7)		Si2	O23	1.623(6)		<NaN1	O,Cl>	2.680
Mn1	O19	2.171(9)		<Si2	O>	1.613				
Mn1	O20	2.140(8)						NaN2	O5	2.584(11)
Mn1	O21	2.149(8)		Si5	O1	1.581(8)		NaN2	O6	2.610(11)
Mn1	O22	2.183(8)		Si5	O2	1.640(6)		NaN2	O10	2.554(9)
<Mn1	O>	2.202		Si5	O5	1.592(7)		NaN2	O12	2.550(11)
				Si5	O13	1.640(6)		NaN2	O13	2.660(11)
Mn1A	O9	2.301(10)		<Si5	O>	1.613		NaN2	O16	2.559(11)
Mn1A	O14	2.327(10)						NaN2	O16	2.898(11)
Mn1A	O19	2.505(18)		Si6	O10	1.632(8)		NaN2	O23	2.713(10)
Mn1A	O20	1.891(14)		Si6	O14	1.582(10)		<NaN2	O>	2.641
Mn1A	O21	1.919(13)		Si6	O23	1.632(8)				
Mn1A	O22	2.508(17)		Si6	O24	1.596(7)		NaN2A	O5	2.436(17)
<Mn1A	O>	2.242		<Si6	O>	1.610		NaN2A	O6	2.821(17)
								NaN2A	O12	2.389(16)

Ce1_2	O1	2.438(9)		Si7	O15	1.639(6)		NaN2A	O13	2.84(2)
Ce1_2	O8	2.438(8)		Si7	O15	1.625(6)		NaN2A	O16	2.442(17)
Ce1_2	O9	2.427(7)		Si7	O17	1.603(7)		NaN2A	O16	2.697(16)
Ce1_2	O14	2.445(7)		Si7	O21	1.588(6)		NaN2A	O25	2.82(4)
Ce1_2	O20	2.350(8)		<Si7	O>	1.614		<Na2A	O,H ₂ O>	2.635
Ce1_2	O21	2.340(8)								
<Ce1_2	O>	2.406		Si8	O12	1.595(7)		NaN3	O3	3.012(10)
				Si8	O13	1.625(6)		NaN3	O8	2.392(8)
Na1_2	O1	2.11(2)		Si8	O18	1.635(6)		NaN3	O9	2.581(10)
Na1_2	O8	2.13(2)		Si8	O19	1.603(8)		NaN3	O11	2.982(10)
Na1_2	O9	2.431(13)		<Si8	O>	1.614		NaN3	O20	2.953(9)
Na1_2	O14	2.408(13)						NaN3	O22	2.423(8)
Na1_2	O20	2.61(2)		Si9	O6	1.636(6)		NaN3	O27	2.55(2)
Na1_2	O21	2.56(2)		Si9	O6	1.638(6)		NaN3	O27	2.68(2)
<Na1_2	O>	2.377		Si9	O16	1.589(6)		<NaN3	O,OH>	2.697
				Si9	O20	1.588(6)				
Mn2_1	O1	2.216(10)		<Si9	O>	1.612		NaN3A	O3	3.07(4)
Mn2_1	O8	2.181(9)						NaN3A	O8	2.75(4)
Mn2_1	O19	2.195(9)		Si10	O2	1.659(6)		NaN3A	O11	3.04(4)
Mn2_1	O22	2.165(8)		Si10	O7	1.586(8)		NaN3A	O22	2.78(4)
Mn2_1	O27	2.61(3)		Si10	O9	1.595(8)		NaN3A	O27	2.38(4)
<Mn2_1	O,OH>	2.273		Si10	O18	1.637(7)		NaN3A	O27	2.30(4)
				<Si10	O>	1.620		NaN3A	Cl28	3.03(5)
Mn2_2	O1	2.20(2)						<NaN3A	O,OH,Cl>	2.76
Mn2_2	O8	2.42(3)		SiM3	O7	1.580(11)				
Mn2_2	O19	2.16(3)		SiM3	O7	1.580(11)		NaN4	O1	2.380(9)
Mn2_2	O22	2.35(3)		SiM3	O7	1.580(11)		NaN4	O5	3.013(14)
<Mn2_2	O>	2.28		SiM3	O30	1.63(3)		NaN4	O12	2.975(14)
				<SiM3	O,OH>	1.592		NaN4	O14	2.578(11)
Mn2_3	O1	2.44(4)						NaN4	O19	2.428(8)
Mn2_3	O8	2.22(2)		SiM4	O24	1.697(9)		NaN4	O21	2.972(10)
Mn2_3	O19	2.32(2)		SiM4	O24	1.697(9)		NaN4	O25	3.024(14)
Mn2_3	O22	2.13(3)		SiM4	O24	1.697(9)		NaN4	O26	2.81(2)

Mn2_3	O27	2.00(4)		SiM4	O26	1.46(4)		<NaN4	O,OH,H ₂ O>	2.773
<Mn2_3	O,OH>	2.19		<SiM4	O,OH>	1.638				
								NaN4A	O1	2.51(5)
NbM3	O7	1.715(9)		SiM4A	O24	1.572(11)		NaN4A	O14	2.20(7)
NbM3	O7	1.715(9)		SiM4A	O24	1.572(11)		NaN4A	O19	2.59(5)
NbM3	O7	1.715(9)		SiM4A	O24	1.572(11)		NaN4A	O24	3.06(9)
NbM3	O27	1.96(2)		SiM4A	O29	1.63(3)		NaN4A	O26	2.39(5)
NbM3	O27	1.96(2)		<SiM4A	O,OH>	1.587		<NaN4A	O,OH>	2.55
NbM3	O27	1.96(2)								
<NbM3	O>	1.837						NaN5	O2	3.16(2)
								NaN5	O7	2.898(19)
								NaN5	O7	3.00(2)
								NaN5	O13	2.579(19)
								NaN5	O18	3.03(2)
								NaN5	O23	3.141(18)
								NaN5	O29	1.97(3)
								NaN5	O30	1.673(17)
								<NaN5	O,OH>	2.681

Prepublished Article

Table 7. Comparative data for amableite-(Ce) and related eudialyte-group minerals with $R\bar{3}$ symmetry.

Mineral	Amableite-(Ce)	Voronkovite	Oneillite	Raslakite	Sergevanite
Idealized formula	$\text{Na}_{15}[(\text{Ce}_{1.5}\text{Na}_{1.5})\text{Mn}_3]\text{Mn}_2\text{Zr}_3\text{Si}[\text{Si}_{24}\text{O}_{69}(\text{OH})_3](\text{OH})_2\cdot\text{H}_2\text{O}$	$\text{Na}_{15}[(\text{Na},\text{Ca})_3\text{Mn}_3]\text{Fe}^{2+}_3\text{Zr}_3\text{Si}_2(\text{Si}_{24}\text{O}_{72})(\text{OH},\text{O})_4\text{Cl}\cdot\text{H}_2\text{O}$	$\text{Na}_{15}[\text{Ca}_3\text{Mn}_3]\text{Fe}_3\text{Zr}_3[\text{SiNb}](\text{Si}_{24}\text{O}_{72})(\text{O},\text{OH},\text{H}_2\text{O})_4\text{Cl}_2$	$\text{Na}_{15}[\text{Ca}_3\text{Fe}_3](\text{Na},\text{Zr})_3\text{Zr}_3[(\text{Si},\text{Nb})\text{Si}](\text{Si}_{24}\text{O}_{72})(\text{OH},\text{H}_2\text{O},\text{O})_4\text{Cl}$	$\text{Na}_{15}[\text{Ca}_3\text{Mn}_3](\text{Na}_2\text{Fe}^{2+})\text{Zr}_3[\text{Si}(\text{Si},\text{Ti})][\text{Si}_{24}\text{O}_{72}](\text{OH},\text{H}_2\text{O},\text{SO}_4)_5$
<i>a</i>, Å	14.1340	14.205	14.2084	14.229	14.2179
<i>c</i>, Å	30.3780	30.265	29.959	30.019	30.3492
<i>V</i>, Å³	5255.6	5289	5237.8	5263.5	5313.11
Strong lines of the powder X-ray diffraction pattern: <i>d</i>, Å (<i>I</i>, %)	11.34 (51)	4.316(85)	11.348 (44)	4.311 (66)	7.12 (70)
	7.06 (76)	3.536(41)	6.021 (36)	4.095 (37)	5.711 (43)
	4.312 (63)	3.221(43)	4.291 (37)	3.209 (58)	4.321 (72)
	3.783 (38)	3.039(41)	3.389 (43)	3.023 (40)	3.551 (39)
	3.538 (43)	2.970(100)	3.150 (35)	2.974 (86)	3.398 (39)
	2.963 (84)	2.848(84)	2.964 (100)	2.853 (100)	2.978 (95)
	2.837 (100)		2.844 (89)		2.855 (100)
Optical data	Biaxial (+) $\alpha \approx \beta = 1.603$ $\gamma = 1.608, 2V = 20^\circ$	Uniaxial (+) $\omega = 1.610$ $\varepsilon = 1.619$	Uniaxial (-) $\omega = 1.6450$ $\varepsilon = 1.6406$	Uniaxial (+) $\omega = 1.608$ $\varepsilon = 1.611$	Uniaxial (+) $\omega = 1.604$ $\varepsilon = 1.607$
Density, g·cm⁻³	2.89 (meas.) 2.899 (calc.)	2.97 (meas.) 2.95 (calc.)	3.20 (meas.) 3.22 (calc.)	2.95 (meas.) 2.945 (calc.)	2.90 (meas.) 2.906 (calc.)
Dominant components at the key sites					
<i>M1a</i>	Ce+Na	Na	Ca	Ca	Ca
<i>M1b</i>	Mn ²⁺	Mn ²⁺	Mn ²⁺	Fe ²⁺	Mn ²⁺
<i>M2</i>	Mn ²⁺	Fe ²⁺	Fe ²⁺	Na	Na
<i>M3</i>	□	Si	Nb	Si	Si
<i>M4</i>	Si	Si	Si	Si	Si

References	This study	Khomyakov <i>et al.</i> , 2009	Johnsen <i>et al.</i> , 1999	Chukanov <i>et al.</i> , 2003	Chukanov <i>et al.</i> , 2020
-------------------	------------	-----------------------------------	---------------------------------	-------------------------------	-------------------------------

Prepublished Article